Modeling and Performance Analysis of a Grid-connected Polycrystalline Silicon Photovoltaic System under the Maritime Climate of El Jadida in Morocco

Sofia Boulmrharj[1,2‡], Mohammed El Ibrahimi[2], Ahmed Louardi[1], Noura Aarich[3], Amin Bennouna[3], Mohamed Bakhouya[2], Mustapha Raoufi[3], Mohamed Monkade[1], Mohammed Zehaf[1], Mohammed Khaidar[1]

[1]University Research Center on Renewable Energies & Intelligent Systems for Energy - Chouaïb Doukkali University, Faculty of Sciences - Avenue of Faculties - El Jadida - Morocco

[2]College of engineering and architecture, LERMA Lab, International University of Rabat, Sala El Jadida, Morocco, 11100

[3]Physics department - Faculty of Sciences Semlalia Marrakech - My Abdellah Avenue - Cadi Ayyad University Morocco.

(boulmrharj@gmail.com, mohammed_elibrahimi@hotmail.com, louardiphysique@gmail.com, aarich.noura@gmail.com, benamin56@gmail.com, Mohamed.bakhouya@uir.ac.ma, raoufi@uca.ac.ma, Monkade@hotmail.com, zehafmohammed@hotmail.com, khaidar.medd@gmail.com)

‡ Corresponding Author; Sofia Boulmrharj, Université Internationale de Rabat Technopolis Rabat-Shore Rocade Rabat-Salé, Tel: +212-530-103-000, Fax: +212-530-10-3000, boulmrharj@gmail.com

Received: 22.04.2020 Accepted:22.05.2020

Abstract- Renewable energy sources (RES) have been extensively deployed as green energy producers for reducing power consumption while diminishing greenhouse emissions. Nowadays, Morocco focuses on RES, especially solar energy due to its abundance, in order to reduce its dependence on fossil products (e.g., coal, oil, gas). The work presented in this article focuses on the modeling, simulation, experimentation and assessment of the performance of a 2.040 kWp grid-connected photovoltaic (PV) system. This latter is based on polycrystalline silicon technology (pc-Si) and installed on the flat roof of the Physics department building of the Faculty of Sciences El Jadida (Latitude 33.22°N, Longitude 8.48°W, Altitude 24 m, and 2.1 km away from the Atlantic Ocean) in Morocco. In fact, the daily and monthly characteristics of the PV system (e.g., power, voltage, current) have been measured, monitored, and analyzed during three years (January 2015-December 2017). Besides, several simulations and experiments have been carried out and the results have been reported and showed that the simulation gives a good approximation of the real-world scenarios. Finally, the monthly average of the produced energy, the efficiency, the final and the reference yields (Y_F and Y_R), the performance ratio (*PR*), and the annual capacity factor (*CF*) of the PV system have been computed and evaluated in order to assess its performance. As a result, the average annual values of the produced energy, the *PR* and the *CF* of our pc-Si PV system were found 1830 kWh/kWp, 79% and 0.21 respectively.

Keywords Grid-connected photovoltaic system, Modeling, Produced energy, System's efficiency, Performance ratio, Performance Analysis.

1. Introduction

The events of the 1960s and 1970s in the Middle East as well as the significant increase in the global energetic consumption over the last years have compelled the whole world, especially the developed countries, to make RES (e.g., solar energy, hydraulic, wind and biomass) a high priority. Therefore, the RES have been extensively deployed as green energy producers in order to diminish greenhouse emissions, primarily caused by using the constantly dwindling fossil fuels

(e.g., coal, oil, gas) as a main energy source (representing 70% of the total energy production) [1]. Nowadays, Morocco, as a sunny country with windy sites, is developing an energy policy geared towards renewable energies and energy efficiency in order to reduce its dependence on fossil products, which is around 90% [1]. This North African country aims to raise the share of renewable energies from 42% in 2020 to 52% in 2030 [2]. For instance, the annual solar irradiation can reach 2500 kWh/m² in this country, especially in the desert, and the average daily global irradiation is around 5 kWh/m² [3]. Therefore, solar energy, especially photovoltaic (PV) panels, is occupying an increasingly larger share amongst the R&D projects in Morocco.

Photovoltaic solar panels have been widely used these last decades for the purpose of converting solar irradiation to useful energy in the form of electricity. They represent one of the most promising energy sources that are able to satisfy the energy consumption needs of a building. Several technologies have been developed when it comes to PV panels, namely, crystalline silicon (c-Si) solar cells, thin film cells and multi-junction cells to name a few. The crystalline silicon solar cells are currently the most manufactured cells worldwide (i.e., more than 90% of the commercially available solar cells) [4]. In fact, there are three types of crystalline silicon solar cells, being monocrystalline silicon (mc-Si), polycrystalline silicon (pc-Si), and amorphous silicon (a-Si) [4]. As for their modeling, there are numerous models that have been proposed and developed for PV cells in order to assess their performance under different meteorological conditions (e.g., temperature, solar irradiation) [5-7]. As a matter of fact, several simulation software tools are available, such as, PVSYST, HOMER, PVPLANNER, System Advisor Model (SAM), which could simulate PV systems and estimate its production and performance [8]. On a related note, the performance of PV systems is principally affected by several parameters, such as, the technology of the PV modules and the weather conditions (especially the solar irradiation and the temperature) [9-11]. Thus, several studies have been conducted in order to assess the behavior and the performance of PV systems under different conditions [11-19]. Some of these studies focused on the impact of several parameters on the efficiency of a single PV module's technology [11, 12], while others assessed the performance of different PV installations that are connected to the grid [13-19].

The work presented in this article is a part of two ongoing R&D projects. The first project, named MIGRID (USAID, PEER program, 2017-2020), aiming at deploying Micro-Grid (MG) systems in buildings. The main aim of this project is to investigate dimensioning and context-driven control approaches for RES integration in energy efficient buildings [6, 7, 20-22]. The second project is a large study conducted within the framework of the PROPRE.MA (PROductivité Photovoltaïque à l'échelle REgionale dans tout le Maroc) project that has lasted more than 3 years (2014-2017), financed by IRESEN and supervised by the Faculty of Sciences Semlalia Marrakech (FSSM). This program is conducted in collaboration with 21 university centers in Morocco [23, 24]. One of the objectives of this project is to map the efficiency and the productivity of three technologies of PV modules (polycrystalline silicon, monocrystalline silicon, amorphous silicon) in 20 different sites in Morocco (i.e., under various weather conditions). Thus, an acquisition platform has been designed and deployed in order to collect the PV system's data and the meteorological data with a sampling time of 5 minutes. The access to this data is done via a Bluetooth modem or transmitted via Ethernet or internet network [25].

The main aim of this article is the modeling, simulation and evaluation of the performance of a deployed 2.040 kWp grid-connected PV system, based on polycrystalline silicon technology (pc-Si) and installed on the flat roof of the Physics Department Building of the Faculty of Sciences El Jadida (Latitude 33.22°N, Longitude 8.48°W, Altitude 24 m, and 2.1 km away from the Atlantic Ocean's coast) in Morocco, during three years (January 2015 - December 2017). Therefore, the modeling of each component of the system has been performed and the simulation of the whole system has been carried out under MATLAB in order to estimate and assess the behavior of the system under various conditions. Besides, the daily and monthly characteristics of the PV system (e.g., power, voltage, current) have been measured, monitored, and analyzed during the three-year duration. This data as well as the weather data [26, 27] have been used in order to compute some important performance indicators (e.g., the total produced AC energy (E_{AC}) by the PV system, the system's efficiency (η_{syst}), the final yield (Y_F) and the performance ratio (PR)). Then, the simulations and the experiments have been carried out under the same conditions in order to compare them for the aim of validating the developed models, so they could be used to size, simulate, and assess the behavior of any PV system before its deployment.

The remainder of this article is structured as follows. The deployed Grid-Connected PV (GCPV) system is described in Section 2. Section 3 puts more emphasis on the modeling of the grid-connected PV system together with its validation using the simulation and experimental results over one day. Section 4 presents the simulation and experimental results over three successive years as well as the performance analysis of the grid-connected PV system. Finally, conclusions and perspectives are given in Section 5.

2. GCPV System's Description

The grid-connected pc-Si PV system, which is composed of 8 PV modules and an inverter, is installed on the flat roof of the Physics department building of the Faculty of Sciences El Jadida in Morocco. In fact, the 8 PV modules (Fig. 1) with 255 Wp for each module (Table 1 provides more PV module's characteristics) are oriented due south with a tilt angle of 30°, which is considered to be close to the optimal tilt in order to generate the maximum amount of energy. Being a Direct Current (DC), the produced electricity by the PV modules needs to be converted into an Alternative Current (AC), which is done using a DC/AC inverter (Fig. 2 (a)). This electricity is then fed to the internal electrical network (220 V, 50 Hz) of the faculty. The inverter used in this installation, which is manufactured by SMA type Sunny boy 2000HF-30, has been described with more details by authors in [24]. Furthermore, in order to collect the PV system's data during the three years, the system has been installed since December 2014 together

with an acquisition platform composed of various sensors (e.g., voltage sensor, current sensor) and electronic cards. The data is collected with a recording interval of 5 minutes. This acquired data can be accessed via a Bluetooth modem or transmitted via Ethernet or internet network.

Fig. 1. The 8 pc-Si PV panels.

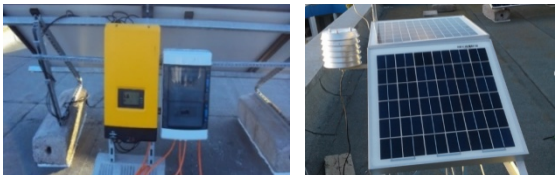

(a) **(b)**

Fig. 2. (a) The DC/AC inverter, and (b) The deployed weather station.

Table 1. PV module's characteristics

Characteristics	Values
Trade Mark	Solar World
Model	Sun module plus
Solar Cell number	60
Maximum Power At STC (P_{mpp})	255 W
Maximum Voltage (V_{mpp})	30.9 V
Maximum Current (I_{mpp})	8.32 A
Open Circuit Voltage (V_{oc})	38 V
Short Circuit Current (I_{sc})	8.88 A
Dimensions	1676 * 1001 * 31 mm^3
Weight	18 kg

On another note, the climate of El Jadida is maritime and the city is constantly swept by the prevailing winds from the north with significant relative humidity. Moreover, the temperature is moderate due to the freshness of the Atlantic Ocean. In order to collect these meteorological data, a weather station has been recently deployed onsite [25]. This station (Fig. 2(b)) is composed of: i) a temperature sensor so as to capture the ambient temperature, ii) a Pt100 temperature sensor for measuring the temperature of the PV module, iii) an anemometer for measuring the wind's speed, iv) a wind vane in order to determine the wind direction, v) two small PV panels (20 W each) where one of them is tilted by 30° and the other is horizontal in order to determine the local solar irradiation, and vi) a processing unit (PC-duino and Raspberry Pi) aiming to collect, process and store measured data.

In fact, the in-plane and horizontal irradiances are measured using the two small PV panels (20 W each) where each one is connected to a shunt resistor, with a small value of about 0.5 Ω, in order to make sure that the PV modules operate near the short circuit condition. Actually, the voltage across the shunt resistor is measured, and using the ohm's law, the short circuit current, which is proportional to the incident solar irradiance, is determined and then corrected in order to take into consideration the variation of the PV module' current with cell temperature. The values of the incident solar irradiance are validated using a pyranometer, which is calibrated in IRESEN laboratories (more details are given in [25]). Therefore, the incident solar irradiance (G) are computed using Eq. (1), where β being the sum of the temperature coefficients of the PV module's short circuit current and the shunt resistor, T_a represents the ambient temperature (°C), T_{ref} stands for the ambient temperature in standard test conditions (°C), γ being the thermal resistor of the PV module (m²/W·K), V_{sh} represents the voltage across the shunt resistor (V), and S_{ref} being the sensibility factor (V/W/m²) [25].

$$G = \frac{-[1+\beta(T_a-T_{ref})]+\sqrt{[1+\beta(T_a-T_{ref})]^2-\frac{4\beta\gamma V_{sh}}{S_{ref}}}}{2\beta\gamma} \quad (1)$$

3. GCPV System's Modeling and Validation

In this section, the modeling of the deployed grid-connected PV system has been performed, and the simulation has been carried out under MATLAB using similar experimental conditions (e.g., ambient temperature, solar irradiation). Then, the simulation and the experimental results have been compared in order to validate the developed models. In fact, the system's components have been modeled and connected in order to build the system's model. Regarding the PV cell's model, a mathematical model of its electrical equivalent circuit has been used in order to simulate its behavior and performance. This electrical equivalent circuit (Fig. 3) is composed of a current source in parallel to a diode, a series resistance and a shunt resistance [6, 28, 29].

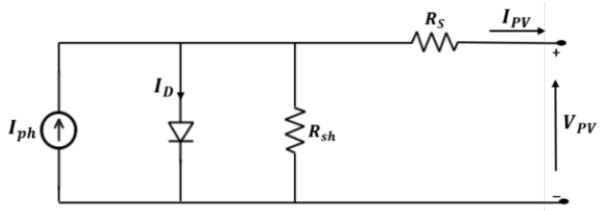

Fig. 3. The single-diode electrical equivalent circuit of the PV cell.

From this electrical circuit, the expression of the $I_{PV} - V_{PV}$ PV cell's characteristic can be derived. It is given using Eq. (2), where I_{ph} being the photocurrent, I_D represents the diode current, and I_{sh} stands for the shunt current [6, 28, 29].

$$I_{PV} = I_{ph} - I_D - I_{sh} \quad (2)$$

The photocurrent is expressed using Eq. (3), where I_r represents the solar irradiance (W/m²), I_{r_0} stands for the irradiance at STC (1000 W/m²), I_{sc} being the cell's short circuit current at STC (A), K_I is the temperature coefficient of the short-circuit current (A/K), T_m represents the cell's temperature (K), and T_{ref} stands for the cell's reference temperature (K) [6, 28, 29].

$$I_{ph} = \frac{I_r}{I_{r_0}} * [\, I_{sc} + K_I(T_m - T_{ref})] \quad (3)$$

Besides, the Shockley diode equation is expressed using Eq. (4), where I_s represents the diode saturation current given by Eq. (5) (A), q being the electron charge ($1.6*10^{-19}$ C), n stands for the diode's ideality factor (it varies between 1.2 and 1.6 for crystalline silicon), K is the Boltzmann constant ($1.38*10^{-23}$ J/K), I_{rs} represents the diode reverse saturation current (A), which is given by Eq. (6), E_g being the cell's semiconductor band-gap energy (eV), V_{oc} represents the cell's open-circuit voltage at STC (V), and N_s being the series cells' number in a module [6, 28, 29].

$$I_D = I_s\left[exp\left(\frac{q\,(V_{PV}+I_{PV}R_s)}{nKT_m}\right)-1\right] \quad (4)$$

$$I_s = I_{rs}\left(\frac{T_m}{T_{ref}}\right)^3 exp\left[\frac{q\,E_g}{n\,K}\left(\frac{1}{T_{ref}}-\frac{1}{T_m}\right)\right] \quad (5)$$

$$I_{rs} = \frac{I_{sc}}{exp\left[\frac{q\,V_{OC}}{N_S\,K\,n\,T_{ref}}\right]-1} \quad (6)$$

Also, the shunt current is expressed using Eq. (7), where R_s and R_{sh} are the series and shunt resistances respectively [6, 28, 29].

$$I_{sh} = \frac{V_{PV}+I_{PV}\,R_S}{R_{sh}} \quad (7)$$

Finally, Eq. (2) can be expressed for a PV module using Eq. (8), where N_p being the number of parallel cells in a module [6, 28, 29].

$$I_{PV} = N_p I_{ph} - N_p I_s\left[exp\left(\frac{q\left(\frac{V_{PV}}{N_S}+\frac{I_{PV}R_S}{N_p}\right)}{nKT_m}\right)-1\right] - \frac{\frac{N_p V_{PV}}{N_S}+I_{PV}\,R_S}{R_{sh}} \quad (8)$$

Figure 4 presents the flowchart diagram of the simulated model, in which we clearly present the steps followed in order to compute the PV module's current, voltage, power, energy and efficiency.

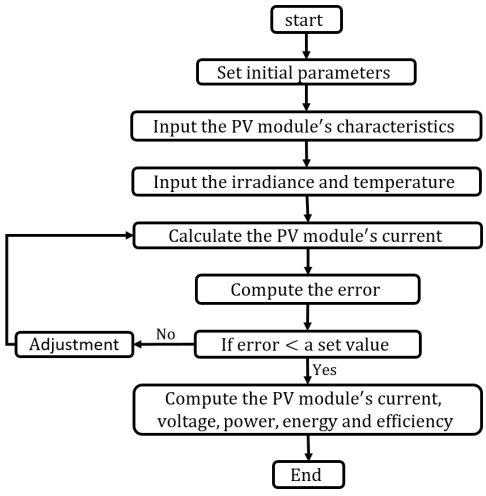

Fig. 4. The flowchart diagram of the simulated model.

As for the inverter, it is worth noting that its efficiency depends on the solar irradiation reaching the surface of the PV panels. For this and using the experimental results of the three years, the efficiency of the inverter was taken as presented in Table 2 in our simulations. Actually, in order to validate the system's model, an experiment has been carried out on the 6th of May 2017, where the produced powers and energies were compared to their simulated counterparts (for the same day, geographical location and weather conditions). Figure 5 depicts the solar irradiation reaching the surface of the PV modules as well as the measured temperature of the PV module. We observe that the solar irradiation can reach more than 900 W/m² around midday in this site, which is very significant, and the temperature is moderate due to the freshness delivered by the Atlantic Ocean. Moreover, Fig. 6 illustrates the experimental and the simulation results of the DC power generated by the PV panels during 24 hours. We observe that before 5 AM and after 7 PM (sunrise and sunset respectively), there is no power production since no solar irradiation is received by the PV panels. However, after 5 AM, the power production increases until midday where the power of the 8 PV panels reaches more than 1.8 kW for both the simulation and the experiment, and then declines until 7 PM.

Table 2. Inverter's efficiency in function of the irradiation

Solar irradiation (W/m²)	Inverter's efficiency (%)
Solar irradiation ≤ 25	0
25 < Solar irradiation ≤ 70	68
70 < Solar irradiation ≤ 100	75
100 < Solar irradiation ≤ 200	85
200 < Solar irradiation ≤ 300	92
300 < Solar irradiation ≤ 400	93
400 < Solar irradiation ≤ 500	94
500 < Solar irradiation	95

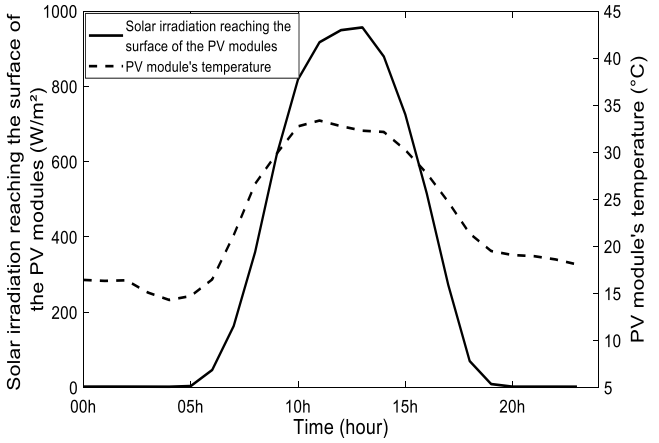

Fig. 5. The solar irradiation on the surface of the PV modules (W/m²) and the measured PV module's temperature (°C).

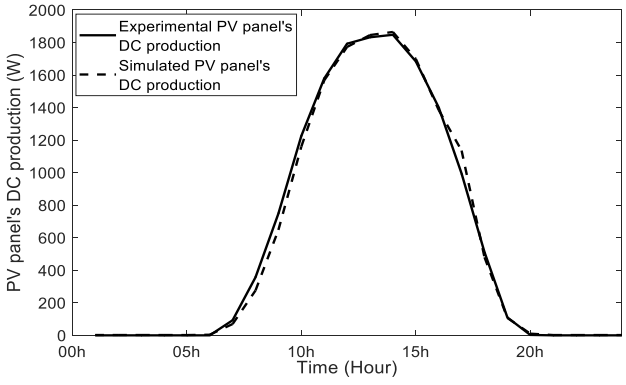

Fig. 6. The experimental/simulated DC production (W).

Furthermore, Fig. 7 depicts the simulation and the experimental results of the AC power produced by the PV system during 24 hours. We can clearly observe that the DC power produced by the PV system has decreased, which is caused by the inverter's efficiency. This latter, which is depicted in Fig. 8, shows that it is around 95% when the solar irradiation is superior to 500 W/m², between 70% and 95% when the solar irradiation is less than 500 W/m², and 0% when there is no solar irradiation. From these results, we can conclude that the efficiency of the inverter is significantly dependent on the solar irradiation.

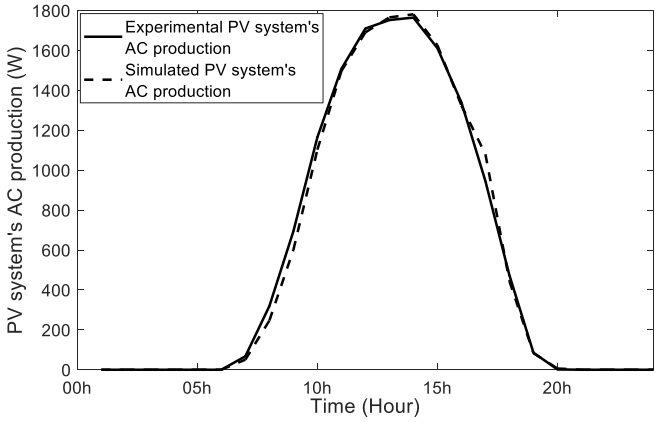

Fig. 7. The experimental/simulated AC production (W).

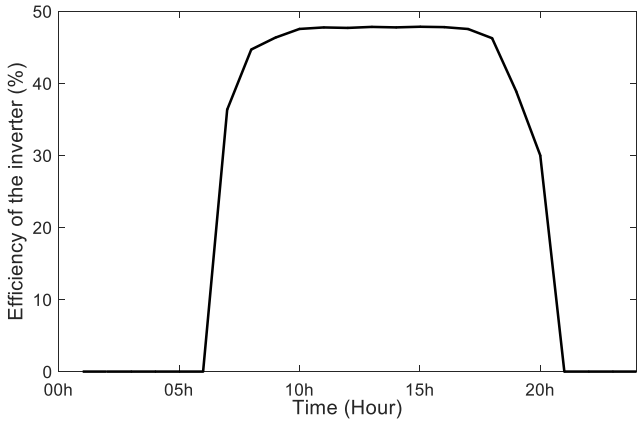

Fig. 8. The inverter's efficiency (%).

Table 3. The daily energy as well as the relative error

	Ours	[30]	[31]
Measured daily energy (kWh)	13.44	--	--
Simulated daily energy (kWh)	13.3	--	--
Relative error (%)	1.04	6	3.63

Besides, as depicted in Table 3, we have computed the energy produced by the PV system (≈ 13.44 kWh for the experiment and ≈ 13.3 kWh for the simulation). Therefore, the error between the simulation and the experiment, which is calculated using Eq. (9), is approximately equal to 1.04% (Table 3). Besides, when comparing this value with relative errors of other studies from the literature (see Table 3), we can conclude that our simulated model gives a better approximation of the real-world scenarios, with a slight error.

$$\varepsilon = \left|\frac{E_{exp}-E_{sim}}{E_{exp}}\right| * 100 \quad (9)$$

4. Performance Analysis of the GCPV System

The evaluation of a generator's (i.e., different types of generators powered with oil, gas, coal or renewable energy) performances is achieved through an estimation of the ratio between its production during a given period (e.g., day, month, year) and the maximum theoretical energy, which it can yield during the same period. In fact, the total generated AC energy (E_{AC}), the efficiency (η_{syst}), the final yield (Y_F), the reference yield (Y_R), the performance ratio (PR), and the capacity factor (CF) are the main performance indicators that provide an overview of the PV system's performances under various operating conditions, since its production is significantly affected by several parameters (e.g., the intermittent solar irradiation, the ambient temperature). Table 4 presents the simulation and the experimental data for the different performance indicators of our PV system as well as the weather data over the three years.

4.1. AC Produced Energy

The total daily ($E_{AC,d}$) and monthly ($E_{AC,m}$) AC energy generated by the PV system are calculated using Eqs (10) and (11) [32]:

$$E_{AC,d} = \sum_{t=1}^{t=288} E_{AC,t} \quad (10)$$

$$E_{AC,m} = \sum_{d=1}^{i=N} E_{AC,d} \quad (11)$$

where N is the number of days of a month and t is the number of 5-minute intervals in a whole day. In fact, the PV module's temperature is needed in order to simulate the behavior of the PV system over the three years and calculate the produced energy. However, we do not have its measured data over the three years because we have had some communication issues. Thus, it ($T_m(°C)$) has been computed using the empirical equation (Eq. 12) proposed by [9].

$$T_m = 0.943 * T_a + 0.028 * G_m - 1.528 * V_w + 4.3 \quad (12)$$

where T_a is the ambient temperature (°C), G_m is the solar irradiation (W/m²), and V_w is the wind speed (m/s). Figure 9 (a, b, c) depicts the data used for calculating the PV module's temperature, which are the ambient temperature, the solar irradiation and the wind speed. Actually, during the summer months in El Jadida, the days are warm and humid, and the winds are cool with generally strong speeds (reaching 7 m/s), contributing to a reduction in the panels' temperatures. As an example, we estimated the panels' temperature using Eq. (12) for V_w = 7 m/s, G_m = 800 W/m² and T_a = 27 °C. The panels' temperature was found to be 41.4 °C. This latter has the same order of magnitude as the temperature measured experimentally at the back of the PV panels, which validated this empirical model.

Table 4. Simulated and experimental data of the system's performance indicators and the weather data, with $E_{AC,sim}$ and $E_{AC,exp}$: Simulated and experimental energy (kWh/kWp), I_{rr}: Monthly solar irradiation (kWh/m²), T_{amb}: Ambient temperature (°C), V: Wind speed (m/s), $I_{rr,day}$: Monthly average daily solar irradiation (kWh/m²/day), $\eta_{syst,sim}$ and $\eta_{syst,exp}$: Simulated and experimental system's efficiency (%), $Y_{F,sim}$ and $Y_{F,exp}$: Simulated and experimental final yield (kWh/kWp-day), Y_R: Reference yield (hour), PR: Performance ratio PR (%)

Month	$E_{AC,sim}$	$E_{AC,exp}$	I_{rr}	T_{amb}	V	$I_{rr,day}$	$\eta_{syst,sim}$	$\eta_{syst,exp}$	$Y_{F,sim}$	$Y_{F,exp}$	Y_R	PR
Jan_15	135.31	118.14	159.84	20	3.89	5.16	12.92	12.21	4.36	3.86	5.16	74.93
Feb_15	139.55	132.55	164.01	18	3.89	5.86	12.99	12.64	4.98	4.79	5.86	81.93
Mar_15	181.89	155.97	211.66	18	4.45	6.83	13.12	11.73	5.87	5.10	6.83	74.70
Apr_15	175.13	163.31	204.77	21	5.56	6.82	13.06	12.32	5.84	5.51	6.82	80.85
May_15	194.41	184.67	227.63	21	5.83	7.34	13.04	12.75	6.27	6.03	7.34	82.24
Jun_15	183.79	171.49	215.88	23	6.67	7.19	12.99	13.09	6.12	5.79	7.19	80.53
July_15	196.39	181.46	229.93	28	6.67	7.42	13.04	12.87	6.33	5.93	7.42	80
Aug_15	183.44	163.27	214.91	27	6.94	6.93	13.03	12.20	5.92	5.34	6.93	77.01
Sep_15	175.71	164.11	205.44	27	6.39	6.85	13.06	12.67	5.85	5.54	6.85	80.97
Oct_15	148.14	134.13	174.81	26	6.67	5.64	12.94	12.01	4.78	4.38	5.64	77.78
Nov_15	154.28	140.45	181.02	21	5.56	6.03	13.01	12.83	5.14	4.74	6.03	78.65
Dec_15	131.22	114.61	155.73	19	3.89	5.02	12.86	12.55	4.23	3.74	5.02	74.60
Jan_16	129.44	129.08	163.26	17	4.44	5.27	12.10	12.27	4.17	4.22	5.27	80.15
Feb_16	133.57	131.55	167.34	16	4.72	5.98	12.19	12.50	4.77	4.59	5.98	76.94
Mar_16	180.64	175.43	220.15	20	5.28	7.10	12.53	12.55	5.82	5.73	7.10	80.78
Apr_16	184.22	178.43	224.43	21	5.56	7.48	12.53	12.30	6.14	6.03	7.48	80.59
May_16	174.58	168.87	215.16	23	6.39	6.94	12.39	12.41	5.63	5.52	6.94	79.56
Jun_16	176.81	171.40	217.99	24	5.83	7.27	12.38	12.68	5.89	5.79	7.27	79.70
July_16	172.22	162.96	213.16	26	5.56	6.87	12.33	12.86	5.55	5.32	6.87	77.50
Aug_16	184.46	168.98	225.81	26	5.56	7.28	12.47	12.76	5.95	5.52	7.28	75.86
Sep_16	174.83	166.66	213.73	26	5.28	7.12	12.49	12.33	5.82	5.63	7.12	79.05
Oct_16	144.79	129.84	180.62	25	4.72	5.83	12.24	12.42	4.67	4.24	5.83	72.87
Nov_16	120.62	120.13	153.16	22	4.72	5.10	12.02	12.09	4.02	4.06	5.10	79.52
Dec_16	125.21	124.57	158.27	22	3.89	5.10	12.08	12.33	4.04	4.07	5.10	79.78
Jan_17	120.12	127.23	154.66	17	4.72	4.99	11.86	12.02	3.87	4.16	4.99	83.40
Feb_17	121.58	112.99	143.45	17	5.83	5.12	12.94	12.03	4.34	4.09	5.12	79.85
Mar_17	171.78	170.16	212	18	6.39	6.84	12.37	12.76	5.54	5.56	6.84	81.36
Apr_17	177.34	175.67	218.38	22	6.39	7.28	12.40	12.55	5.91	5.93	7.28	81.55
May_17	180.68	172.98	223.84	23	6.67	7.22	12.32	12.07	5.83	5.65	7.22	78.34
Jun_17	168.23	161.54	210.14	25	7.22	7	12.22	13.04	5.61	5.45	7	77.93
July_17	180.92	169.23	224.20	25	7.22	7.23	12.32	12.39	5.83	5.53	7.23	76.52
Aug_17	179.69	161.24	222.12	26	7.5	7.16	12.35	12.19	5.79	5.27	7.16	73.59
Sep_17	166.65	162.67	206.65	24	6.67	6.89	12.31	12.51	5.55	5.49	6.89	79.80
Oct_17	167.26	152.37	206.78	25	5.56	6.67	12.35	12.84	5.39	4.98	6.67	74.70
Nov_17	136.39	136.60	160.91	21	5.83	5.36	12.94	12.73	4.54	4.61	5.36	86.06
Dec_17	137.56	136.44	162.97	17	6.11	5.26	12.89	12.70	4.44	4.46	5.25	84.87

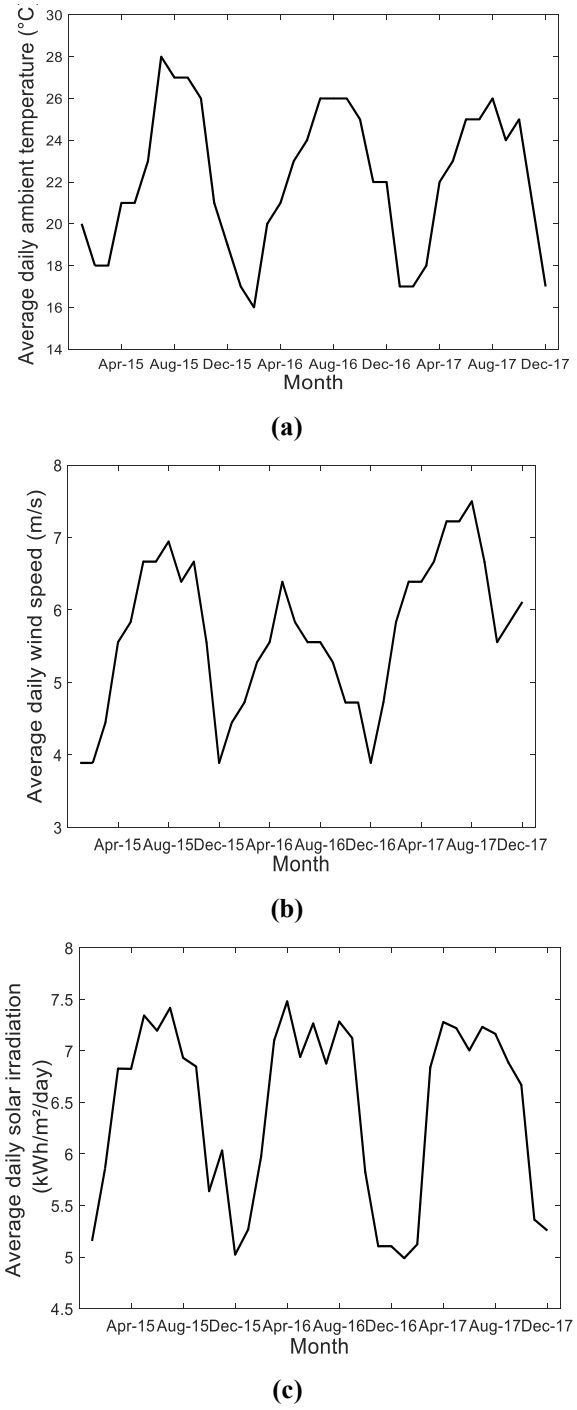

Fig. 9. (a) Monthly average daily ambient temperature (°C), (b) Monthly average daily wind speed (m/s), and (c) Monthly average daily solar irradiation (kWh/m²/day) over the monitoring period (January 2015 – December 2017).

Once the PV module's temperature was estimated, the PV system has been simulated and the produced energy has been computed. From the results depicted in Fig. 10 (a, b, and c) and Table 4, the annual solar irradiation reaching the surface of the PV panels (with a tilt of 30°) is 2345.67, 2353 and 2346.12 kWh/m² for the three years 2015, 2016 and 2017 respectively, with an average value of 2348.26 kWh/m². From the same figure, we can conclude that the patterns of these magnitudes (the simulation and the experimental monthly energy produced by the PV panels and the solar irradiation reaching the surface of the PV system (tilted by 30°)) are similar. Furthermore, we observe that the monthly energy produced by the PV panels varies between a minimum value of ≈ 112.99 kWh/kWp, which corresponds to February 2017 (winter period) with a solar irradiation of ≈ 143.45 kWh/m², and a maximum value of ≈ 184.67 kWh/kWp, which corresponds to May 2015 (spring period) with a solar irradiation of ≈ 227.63 kWh/m². Moreover, the annual error between the simulation and the experimental results is approximately equal to 9.8%, 3.9% and 4.6% for the three years 2015, 2016 and 2017 respectively, with an average value of about 6.1%. The difference between this error and the one computed when validating the model is caused by the fact that the solar irradiation data used for the three years was provided by the PVGIS website, which gives an approximation of the real irradiation, whilst the data used for the validation was in fact measured. Consequently, we can conclude that the grid-connected PV system's model is validated for the three years, and that it gives good estimations of the real-world scenario with a slight error (an average annual error of about 6.1%).

Figure 11 depicts the simulated and experimental average monthly energy produced by the PV system over the span of three years, in addition to the three-year average solar irradiation reaching the surface of the same PV panels. The year can be divided into two periods (energy-wise): from October to February, with an average produced energy of about 129 kWh/kWp, and from March to September, with an average produced energy of about 170 kWh/kWp. After computing the average annual energy produced by the PV system, which we found equal to 1830 kWh/kWp, we conclude that the deviation from the average annual energy generated by the PV system is -6 kWh (0.3%), -2 kWh (0.1%), and 9 kWh (0.5%) for the years 2015, 2016 and 2017 respectively. Besides, we observe that the simulated results are mostly greater than the experimental results. This can be provoked by not using measured data for the PV module's temperature over the three years (i.e., it is simulated using Eq. (12)), since we have had some communication issues, or an overshooting of one of the initial parameters (e.g., ideality factor).

On another note, Table 5 presents the daily and annual relative errors of our experiment as well as others from the literature. We observe that the average annual error of our experiment has the same order of magnitude as the ones of the other studies. From this comparison, we can conclude that the developed models gave good approximation of real-world scenarios.

Table 5. The daily and annual relative errors

Relative error (%)	Ours	[33]	[34]
Daily error	1.04	--	--
Average annual error	6.1	6	4.74

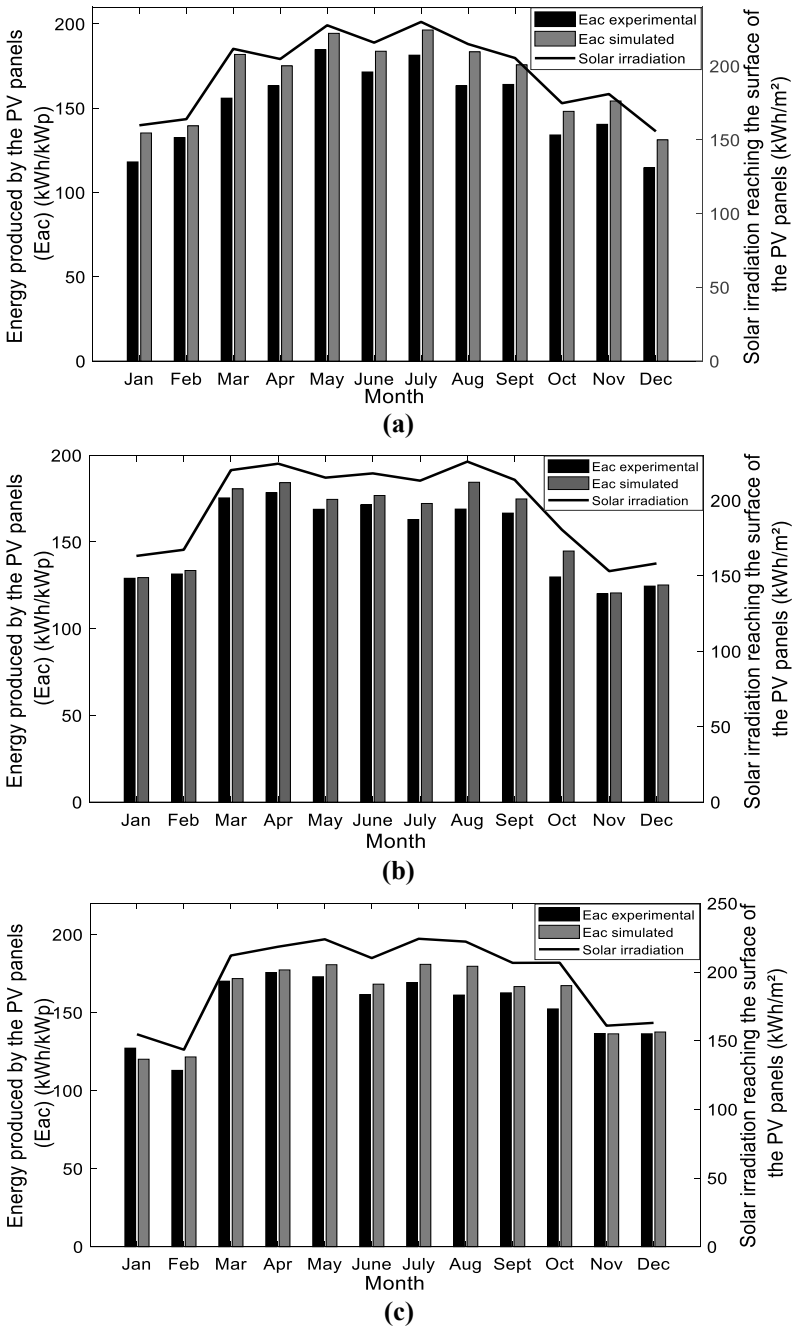

Fig. 10. The simulated/experimental monthly energy produced by the PV panels (kWh/kWp) and the solar irradiation reaching the surface of the PV panels (kWh/m²) during (a) 2015, (b) 2016, and (c) 2017.

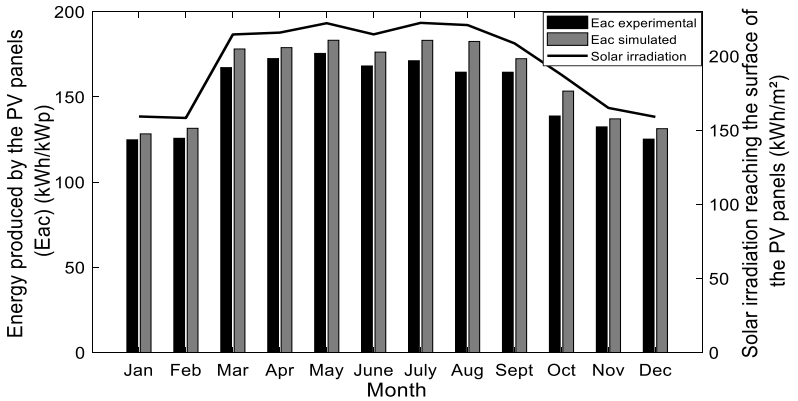

Fig. 11. The three-year average of the simulated/experimental monthly energy produced by the PV panels (kWh/kWp) and the three-year average solar irradiation reaching the surface of the PV panels (kWh/m²).

4.2. System's Efficiency

The instantaneous PV system's efficiency (η_{syst}) is calculated using Eq. (13), in which G_m stands for the in-plane solar irradiation (kW/m²), P_{AC} represents the generated AC power (kW) and A_a denotes the PV array's area (m²).

$$\eta_{syst} = \frac{P_{AC}}{G_m \times A_a} * 100 \quad (13)$$

Therefore, the monthly overall PV system efficiency ($\eta_{syst,m}$) is calculated using Eq. (14) [35], where $\bar{E}_{AC,d}$ represents the monthly average daily produced AC energy (kWh), $\bar{G}_{t,d}$ being the monthly average daily in-plane (in this case tilted by 30°) solar irradiation (kWh/m²), and A_a, which is equal to 13.41 m², stands for the PV array's area.

$$\eta_{syst,m} = \frac{\bar{E}_{AC,d}}{\bar{G}_{t,d} \times A_a} * 100 \quad (14)$$

Figure 12 depicts the simulated and the experimental monthly AC energy produced by the PV panels as well as the simulated and the experimental monthly efficiency of the PV system over the monitoring period. From these results, we can conclude that the simulation and experimental results are in agreement, which validates the developed models. Moreover, the average system's efficiency has dropped from 15% (the efficiency mentioned by the manufacturer) to 12.5% (the simulated and experimental efficiency). This drop is mainly caused by the weather conditions and/or the frequency of cleaning the PV modules. In fact, in our case, a weekly cleaning has been performed. However, the deposit of very fine dust is inevitable, especially for the period from June to September, which is characterized by its dry weather. Actually, the drop in the PV system's efficiency can also be observed in other performance indicators, such as, the final yield, the reference yield, and the performance ratio.

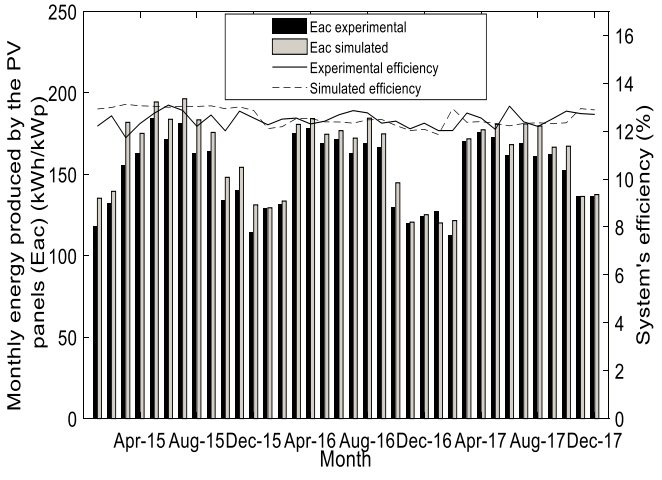

Fig. 12. The simulated/experimental monthly energy produced by the PV system (kWh/kWp) as well as the system's efficiency (%) over the monitoring period.

4.3. Final and Reference yields

The final yield (Y_F) is defined (Eq. (15)) as the ratio between the annual, monthly or daily produced AC energy by the PV system ($\bar{E}_{AC}(kWh_{AC})$) and the peak power ($P_{PV,rated}(kW_{DC})$) of the installed PV array at standard conditions (STC), which are 1000 W/m² solar irradiation and 25 °C temperature.

$$Y_F = \frac{\bar{E}_{AC}}{P_{PV,rated}} \quad (15)$$

The annual final yield ($Y_{F,a}$) is given in Eq. (16) [32]:

$$Y_{F,a} = \frac{\bar{E}_{AC,a}}{P_{PV,rated}} \quad (16)$$

where $\bar{E}_{AC,a}$ represents the total annual AC energy generated by the PV system (kWh). Moreover, the daily final yield ($Y_{F,d}$) and the monthly average final yield ($Y_{F,m}$) are given in Eqs (17) and (18):

$$Y_{F,d} = \frac{E_{AC,d}}{P_{PV,rated}} = \frac{E_{AC,m}/N}{P_{PV,rated}} \quad (17)$$

$$Y_{F,m} = \frac{1}{N}\sum_{d=1}^{N} Y_{F,d} \quad (18)$$

where $E_{AC,d}$ represents the total daily AC energy produced by the PV system (kWh), and N being the number of days in a month. Figure 13 illustrates the simulated and the experimental monthly average daily Final Yield (Y_F) of the grid connected PV system over the monitoring period. We observe that the monthly average daily final yield varies between a minimum value of about 3.74 kWh/kWp/day, corresponding to December 2015 (winter period), and a maximum value of about 6.04 kWh/kWp/day, which corresponds to May 2015 (spring period). Besides, the three-year average daily final yield of the PV system is around 5.1 kWh/kWp/day. As a conclusion, the high value of the final yield proves the good performance of the PV system and its capability to generate more energy per day. Furthermore, we can see in Fig. 13 and Table 4 that the simulation and the experimental values of the final yield of the PV system are very close, which led us to conclude that the simulation gives a good estimation of the real world scenario.

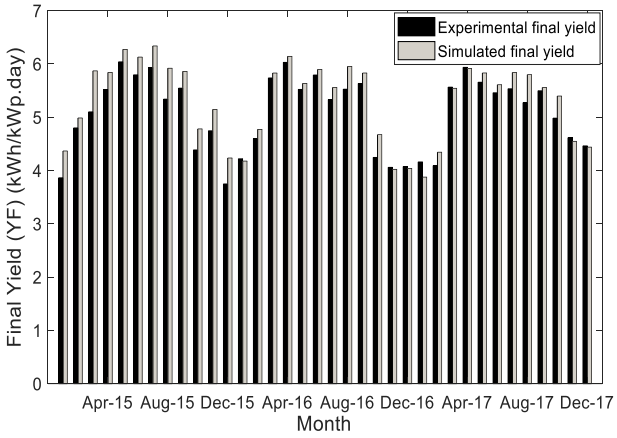

Fig. 13. The simulated/experimental monthly average daily Final Yield (Y_F) (kWh/kWp/day) over the monitoring period.

The reference yield (Y_R) is the ratio between the total in-plane solar irradiation $G_t(kWh/m^2)$ and the total solar radiation on the PV array at STC conditions (G_{STC}=1 (kW/m^2)). Therefore, the reference yield, which corresponds to the number of the peak sun-hours, is calculated using Eq. (19) [35]:

$$Y_R = \frac{G_t}{G_{STC}} \quad (19)$$

Figure 14 depicts the monthly average daily Reference Yield (Y_R) of the grid connected PV system over the monitoring period. We can observe that the monthly average daily reference yield varies between a minimum value of around 5 hours, corresponding to January 2017 (winter period), and a maximum value of around 7.5 hours, which corresponds to April 2016 (spring period). Besides, the three-year average daily reference yield of the PV system is around 6.5 hours. Furthermore, the simulated and the experimental reference yields are the same in our case because we have used the same irradiation in both of them, which is provided by the PVGIS website, since we do not have its real values.

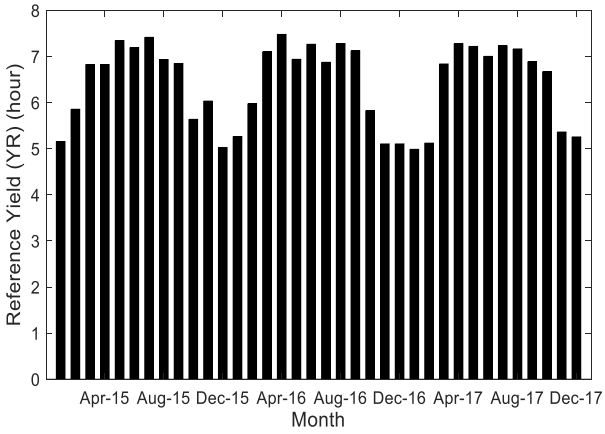

Fig. 14. The monthly average daily Reference Yield (Y_R) (hour) over the monitoring period.

4.4. Performance Ratio

The Performance Ratio (PR) is one of the most important indicators for evaluating the performance of a PV plant. In fact, the performance ratio is the proportion between the actual and the theoretically possible energy production. It provides an indication about the overall losses in the power production of a PV system and depends on numerous parameters, such as, the quality of the cables, the efficiency of DC/DC converter, the efficiency of the inverter. Therefore, the performance ratio is an indicator that could give a detailed inspection of the PV plant so that, for example, soiling of the PV modules could be removed or defective components could be repaired or replaced. It can be expressed as follows (Eq. (20)) [36]:

$$PR = \frac{\eta_{sys}}{\eta_{sys,STC}} = \frac{E_{AC} * G_{STC}}{G_m * P_{DC,STC}} \quad (20)$$

where: $\eta_{sys} = \frac{E_{AC}}{A_a * G_m}$ and $\eta_{sys,STC} = \frac{P_{DC,STC}}{A_a * G_{STC}}$

The performance ratio can be also defined as a fraction between the final and the reference yield of the PV system, and could be expressed as follows (Eq. (21)) :

$$PR = \frac{Y_F}{Y_R} = \frac{E_{real}}{E_{ideal}} \quad (21)$$

where E_{real} represents the energy generated by the PV system during its operation (kWh) and E_{ideal} is the energy generated at rated power (kWh). Figure 15 shows the monthly average daily performance ratio (PR) of the PV system during the monitored 36 months. The performance ratio varies between a minimum value of around 73%, which corresponds to October 2016, and a maximum value of about 86.1%, which corresponds to November 2017. Besides, the three-year average daily performance ratio is around 79%. Therefore, the high value of the performance ratio reveals the good performance and behavior of the PV system during the three years.

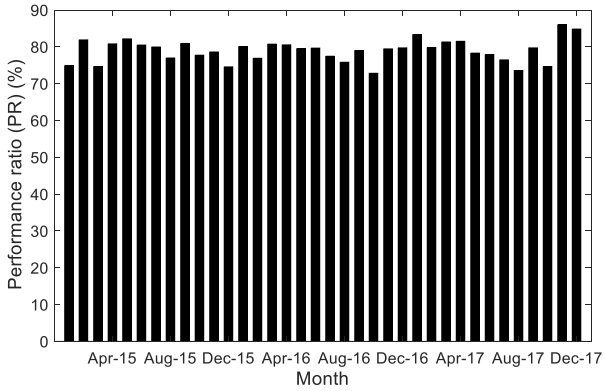

Fig. 15. The monthly average daily Performance Ratio (PR) of the PV system (%) over the monitored period.

4.5. Capacity Factor

The capacity factor CF is defined as the ratio between the actual annual produced energy ($E_{AC,a}$) by the PV system and the amount of energy that this system would generate if it operated at full rated power ($P_{PV,rated}$) for 24 hours per day for a year. Based on this definition, the expression of the CF is given in Eq. (22) [32]. The definition of this performance indicator shows that its expected value cannot be significant because the actual system capacity is bound to the number of sunshine's hours. The average yearly CF of our PV system is approximately 0.21.

$$CF = \frac{Y_{F,a}}{24 \times 365} = \frac{E_{AC,a}}{P_{PV,rated} \times 8760} = \frac{G_m \times PR}{P_{PV,rated} \times 8760} \quad (22)$$

5. Conclusions and Perspectives

This paper presents the results of a study that aimed to model, simulate and evaluate the performance of a 2.040 kWp grid-connected photovoltaic (PV) system. Obtained results showed that the developed models gave good approximation of the real-world scenarios, with a slight error (an average daily and annual errors of about 1.04% and 6.1% respectively). Then, the monthly average of the AC produced energy, the efficiency, the final and the reference yields (Y_F and Y_R), the performance ratio (PR), and the annual capacity factor (CF) of the PV system have been computed and analyzed. In our case, the average annual values of the produced energy, PR and CF are 1830 kWh/kWp, 79% and 0.21 respectively. The high value of the performance ratio revealed the good performance and behavior of the PV system during the full three years. Moreover, we have compared our results to others obtained from other studies in other countries, such as, Germany (850 kWh/kWp [37]), Northern Ireland (876 kWh/kWp [32]), Greece (1337 kWh/kWp [38]), Spain (1361 kWh/kWp [39]) and Kosovo (1330 kWh/kWp [36]). This

comparison showed that the annual energy produced by our PV system, which is standardized to 1 kWp, is higher than those produced in the other countries, even if they have the same order of magnitude as the relatively moderate solar irradiation of our site (El Jadida). This is attributed to the fact that El Jadida has higher wind speed and lower ambient temperature, which help reducing the temperature of the PV modules, and thus increasing their energy production. As a perspective, we will investigate the use of the daily performance ratio of the system as an indicator for detecting any system's flaw.

Acknowledgements

This work was supported by IRESEN, grant number InnoPV.13.PROPRE.MA. It is also partially funded by USAID under the PEER program, grant number 5-398 (2017-2020).

References

[1] Fossil fuel energy consumption (% of total), https://data.worldbank.org/indicator/eg.use.comm.fo.zs?end=2015&start=1960 (Accessed 15 March 2020).

[2] National Energy Strategy, http://giz-energy.ma/energy-context/national-energy-strategy/?lang=en (Accessed 16 March 2020).

[3] H. Othieno, and J. Awange, "Energy resources in Africa, distribution, opportunities and challenges", *Springer,* 2016. https://doi.org/10.1007/978-3-319-25187-5.

[4] O. Ogbomo Osarumen, H. Amalu Emeka, N. N. Ekere, and P. O. Olagbegi, "A review of photovoltaic module technologies for increased performance in tropical climate", *Renewable and Sustainable Energy Reviews, Elsevier*, vol. 75, pp. 1225-1238, 2017. https://doi.org/10.1016/j.rser.2016.11.109.

[5] M. Jazayeri, S. Uysal, and K. Jazayeri, "A Simple Matlab/SIMULINK Simulation for PV Modules Based on One-Diode Model", *HONET, IEEE, Magosa, Cyprus*, pp. 44-50, December 2013. https://doi.org/10.1109/HONET.2013.6729755.

[6] S. Boulmrharj, R. Rabeh, V. Felix, R. Ouladsine, M. Bakhouya, K. Zine-Dine, M. Khaidar, M. Siniti, and R. Abid, "Modeling and dimensioning of grid-connected photovoltaic systems", *In the Proceedings of the IRSEC'17, IEEE, Morocco*, pp. 1-6, December 2017. https://doi.org/10.1109/IRSEC.2017.8477392.

[7] S. Boulmrharj, Y. NaitMalek, A. ElMouatamid, M. Bakhouya, R. Ouladsine, K. Zine-Dine, M. Khaidar, and R. Abid, "Approach for Dimensioning Stand-alone Photovoltaic Systems", *ICEER 2018, Energy Procedia, Czech Republic*, vol. 153, pp. 56-61, 2018. https://doi.org/10.1016/j.egypro.2018.10.058.

[8] Seven Most Popular Solar PV Design and Simulation Software, https://www.linkedin.com/pulse/7-most-popular-solar-pv-design-simulation-software-eslam-allam (Accessed 20 March 2020).

[9] G. TamizhMani, L. Ji, Y. Tang, and L. Petacci, "Photovoltaic module thermal/wind performance: Long -Term Monitoring and Model Development for Energy Rating", *NCPV and Solar Program Review Meeting, Denver, USA*, pp. 936-939, June 2006. https://www.nrel.gov/docs/fy03osti/35645.pdf.

[10] E. Skoplaki, and J. A. Palyvos, "On the temperature dependence of photovoltaic module electrical performance: A review of efficiency/power correlations", *Solar Energy, Elsevier*, 83, pp. 614–624, 2009. https://doi.org/10.1016/j.solener.2008.10.008.

[11] H. Bahaidarah, S. Rehman, A. Subhan, P. Gandhidasan, and H. Baig, "Performance Evaluation of a PV Module under Climatic Conditions of Dhahran, Saudi Arabia", *EEE*, vol. 33(6), pp. 909–929, 2015. https://doi.org/10.1260/0144-5987.33.6.909.

[12] E. Kurt, and G. Soykan, "Performance Analysis of DC Grid Connected PV System Under Irradiation and Temperature Variations", *ICRERA 2019, IEEE*, pp. 702-707, November 2019. https://doi.org/10.1109/ICRERA47325.2019.8996577.

[13] K. Oda, K. Hakuta, Y. Nozaki, and Y. Ueda, "Characteristics evaluation of various types of PV modules in Japan and US", *ICRERA 2016, IEEE*, pp. 977-982, 2016. https://doi.org/10.1109/ICRERA.2016.7884481.

[14] P. C. Babu, S. S. Dash, R. Bayındır, R. K. Behera, and C. Subramani, "Analysis and experimental investigation for grid-connected 10 kW solar PV system in distribution networks", *ICRERA 2016, IEEE*, pp. 772-777, 2016. https://doi.org/10.1109/ICRERA.2016.7884441.

[15] G. Bayrak, and M. Cebeci, "Monitoring a grid connected PV power generation system with labview", *ICRERA 2013, IEEE*, pp. 562-567, 2013. https://doi.org/10.1109/ICRERA.2013.6749819.

[16] H. Rezk, M. R. Gomaa, M. A. Mohamed, and M. J. Al shammri, "Energy Performance Analysis of On-Grid Solar Photovoltaic System-a Practical Case Study", *IJRER*, vol. 9(3), pp. 1292-1301, 2019. https://www.ijrer.com/index.php/ijrer/article/view/9629/pdf.

[17] V. P. Singh, B. Ravindra, V. Vijay, and M. S. Bhatt, "A comparative performance analysis of C-Si and A-Si PV based rooftop grid tied solar photovoltaic systems in Jodhpur", *ICRERA 2014, IEEE*, pp. 250-255, 2014. https://doi.org/10.1109/ICRERA.2014.7016565.

[18] D. A. Quansah, M. S. Adaramola, G. K. Appiah, and I. A. Edwin, "Performance analysis of different grid-connected solar photovoltaic (PV) system technologies with combined capacity of 20 kW located in humid tropical climate", *International Journal of Hydrogen Energy, Elsevier*, vol. 42(7), pp. 4626-4635, 2017. http://dx.doi.org/10.1016/j.ijhydene.2016.10.119.

[19] A. Ghouari, "Data monitoring and performance analysis of a 1.6 kWp grid connected PV system in Algeria", *IJRER*, vol. 6(1), pp. 34-42, 2016. https://pdfs.semanticscholar.org/a776/e232c40e1ca631ce72ce72801d78d6699879.pdf.

[20] M. Bakhouya, Y. NaitMalek, A. Elmouatamid, F. Lachhab, A. Berouine, S. Boulmrharj, R. Ouladsine, V. Felix, K. Zinedine, M. Khaidar, and N. Elkamoune, "Towards a context-driven platform using IoT and big data technologies for energy efficient buildings", CloudTech, pp. 1-5, 2017. https://doi.org/10.1109/CloudTech.2017.8284744.

[21] S. Boulmrharj, Y. NaitMalek, A. Elmouatamid, M. Bakhouya, R. Ouladsine, K. Zine-Dine, M. Khaidar, and M. Siniti, "Battery Characterization and Dimensioning Approaches for Micro-Grid Systems", *Energies*, vol. 12(7), 2019. https://doi.org/10.3390/en12071305.

[22] A. Elmouatamid, Y. NaitMalek, R. Ouladsine, M. Bakhouya, N. Elkamoun, K. Zine-Dine, M. Khaidar, and R. Abid, "Towards a Demand/Response Control Approach for Micro-grid Systems", *CoDIT*, pp. 984-988, 2018. https://doi.org/10.1109/CoDIT.2018.8394951.

[23] A. Bennouna, N. Aarich, N. Erraissi, M. Akhsassi, A. Asselman, A. Barhdadi, L. Boukhattem, A. Cherkaoui, Y. Darmane, A. Doudou, A. El Fanaoui,, H. El Omari, M. Fahoume, M. Hadrami, B. Hartiti, A. Ihlal, M. Khaidar, A. Lfakir, H. Lotfi, K. Loudiyi, M. Mabrouki, D. Moussaid, M. Raoufi, A. Ridah, R. Saadani, I. Zorkani, M. Aboufirass and A. Ghennioui, "Energy performance of 3 silicon-based PV module technologies in 20 sites of Morocco", *Energy for Sustainable Development*, vol. 53, pp. 30-56, 2019. https://doi.org/10.1016/j.esd.2019.09.002.

[24] H. Lotfi, A. Bennouna, D. Izbaim, and M. Neffa, "Performance Analysis of Amorphous Photovoltaic Module Technology in Laâyoune –Morocco", *Journal of Electrical and Electronics Engineering*, vol. 13, pp. 35-42, 2018. https://doi.org/10.9790/1676-1306013542.

[25] N. Erraissi, M. Raoufi, N. Aarich, M. Akhsassi, and A. Bennouna, "Implementation of a low-cost data acquisition system for "PROPRE.MA" project", *Measurement*, vol. 117, pp. 21-40, 2018. http://dx.doi.org/10.1016/j.measurement.2017.11.058.

[26] Photovoltaic geographical information system, https://re.jrc.ec.europa.eu/pvg_tools/fr/tools.html (Accessed 30 March 2020).

[27] El Jadida: Historique Météo, https://www.historique-meteo.net/afrique/maroc/el-jadida/ (Accessed 30 March 2020).

[28] M. Elibrahimi, A. Elmouatamid, M .Bakhouya, K. Feddi, and R. Ouladsine, "Performance Evaluation of Fixed and Sun Tracking Photovoltaic Systems", *IRSEC 2018, IEEE, Rabat, Morocco*, pp. 1-6, December 2018. https://doi.org/10.1109/IRSEC.2018.8702932.

[29] J. A. Gow, and C. D. Manning, "Development of a photovoltaic array model for use in power-electronics simulation studies", *IEEE Proceedings-Electric Power Applications*, vol. 146(2), pp. 193-200, 1999. https://doi.org/10.1049/ip-epa:19990116.

[30] M. Puianu, R. O. Flangea, N. Arghira, and S. S. Iliescu, "PV panel-wind turbine hybrid system modelling", *CSCS*, pp. 636-640, May 2017. https://doi.org/10.1109/CSCS.2017.97.

[31] A. Dolara, S. Leva, and G. Manzolini, "Comparison of different physical models for PV power output prediction", *Solar energy*, vol. 119, pp. 83-99, 2015. https://doi.org/10.1016/j.solener.2015.06.017.

[32] L. Ayompe, A. Duffy, S. McCormack, and M. Conlon, "Measured Performance of a 1.72 kW Rooftop Grid-Connected Photovoltaic System in Ireland", *Energy Conversion and Management,* vol. 52, pp. 816-825, 2011. https://doi.org/10.1016/j.enconman.2010.08.007.

[33] L. Ayompe, "Performance and policy evaluation of solar energy technologies for domestic application in Ireland", thesis report, Technological University Dublin, 2011. https://arrow.tudublin.ie/engdoc/37/.

[34] J. D. Mondol, Y. G. Yohanis, M. Smyth, and B. Norton, "Long-term validated simulation of a building integrated photovoltaic system", *Solar energy*, vol. 78(2), pp. 163-176, 2005. https://doi.org/10.1016/j.solener.2004.04.021.

[35] J. D. Mondol, Y. G. Yohanis, and B. Norton, "The effect of low insolation conditions and inverter oversizing on long-term performance of a grid-connected photovoltaic system", *Progress in Photovoltaics: Research and Applications*, vol. 15(4), pp. 353–368, 2007. https://doi.org/10.1002/pip.742.

[36] V. Komoni, I. Krasniqi, A. Lekaj, and I. Gashi, "Performance analysis of 3.9 kW grid-connected photovoltaic systems in Kosovo", *IREC,* pp. 1-6, 2014. https://doi.org/10.1109/IREC.2014.6826947.

[37] B. Decker, and U. Jahn,, "Performance of 170 grid-connected PV plants in northern Germany-analysis of yields and optimization potentials", *Solar Energy*, vol. 59, pp. 127-133, 1997. https://doi.org/10.1016/S0038-092X(96)00132-6.

[38] E. Kymakis, S. Kalykakis, and T. M. Papazoglou, "Performance analysis of a grid connected Photovoltaic Park on the island of Crete", *Energy Conversion and Management, Elsevier*, vol. 50(3), pp. 433–438, 2009. https://doi.org/10.1016/j.enconman.2008.12.009.

[39] M. Sidrach-de-Cardona, and L. Mora Lopez, "Performance analysis of a grid-connected photovoltaic system", *Energy, Elsevier*, vol. 24(2), pp. 93-102, 1999. https://doi.org/10.1016/S0360-5442(98)00084-X.